PASJ: Publ. Astron. Soc. Japan **58**, 177–186, 2006 February 25

Reliability Checks on the Indo-US Stellar Spectral Library Using Artificial Neural Networks and Principal Component Analysis

Harinder P. SINGH
Department of Physics and Astrophysics, University of Delhi, Delhi 110007, India
hpsingh@physics.du.ac.in
Manabu YUASA and Nawo YAMAMOTO
Research Institute for Science and Technology, Kinki University, Higashi-Osaka, Osaka 577-8502
yuasa@rist.kindai.ac.jp
and
Ranjan GUPTA
Inter-University Center for Astronomy and Astrophysics, Ganeshkhind, Pune 411007, India
rag@iucaa.ernet.in

(Received 2005 October 21; accepted 2005 December 16)

Abstract

The Indo-US coudé feed stellar spectral library (CFLIB) made available to the astronomical community recently by Valdes et al. (2004, ApJS, 152, 251) contains spectra of 1273 stars in the spectral region 3460 to 9464 Å at a high resolution of 1 Å (FWHM) and a wide range of spectral types. Cross-checking the reliability of this database is an important and desirable exercise since a number of stars in this database have no known spectral types and a considerable fraction of stars has not so complete coverage in the full wavelength region of 3460–9464 Å resulting in gaps ranging from a few Å to several tens of Å. We use an automated classification scheme based on Artificial Neural Networks (ANN) to classify all 1273 stars in the database. In addition, principal component analysis (PCA) is carried out to reduce the dimensionality of the data set before the spectra are classified by the ANN. Most importantly, we have successfully demonstrated employment of a variation of the PCA technique to restore the missing data in a sample of 300 stars out of the CFLIB.

Key words: catalogs — methods: data analysis — stars: general

1. Introduction

Automated schemes of data validation and analysis have assumed added significance recently as larger databases are increasingly becoming available in almost all areas of observational astronomy. With the advent of bigger CCD detectors in spectroscopy, the need for having large libraries of stellar spectra at high spectral resolution is also getting fulfilled. Jacoby, Hunter, and Christian (1984, hereafter JHC) made 158 spectra available in the range of 3510–7427 Å at 4.5 Å resolution. Prugniel and Soubiran (2001) published a library of 708 stars using the ELODIE eschelle spectrograph at the Observatoire de Haute-Province that covers a wavelength band of 4100–6800 Å at a resolution of $R = 42000$. Cenarro et al. (2001) have provided a database of 706 stellar spectra in the wavelength region 8350–9020 Å at 1.5 Å resolution and Le Borgne et al. (2003, hereafter STELIB) with 247 spectra in the range of 3200–9500 Å at 3 Å resolution. Moultaka et al. (2004, hereafter ELODIE) compiled 1959 spectra in the range of 4000–6800 Å at a resolution of 0.55 Å.

More recently, Valdes et al. (2004) observed more than 1200 stars with emphasis on broad wavelength coverage (3400–9500 Å) at a resolution of ~ 1 Å (FWHM) at an original dispersion of 0.44 Å per pixel. Their coudé feed stellar spectral library (CFLIB) provides a resolution sufficient to resolve numerous diagnostic spectral features that can be used in the automated parameterization of spectra.

Neural networks are a form of multiprocessor computing system, with simple processing elements with a high degree of inter-connection, simple scalar messaging, and adaptive interaction between elements. In a supervised back propagation algorithm, the network topology is constrained to be feed-forward, i.e., connections are generally allowed from the input layer to the first (and mostly only) hidden layer; from the first hidden layer to the second, …, and from the last hidden layer to the output layer. The hidden layer learns to recode (or to provide a representation for) the inputs. More than one hidden layer can be used. The architecture is more powerful than single-layer networks: it can be shown that any mapping can be learned, given two hidden layers (of units).

Automated schemes like the Artificial Neural Networks (ANN) have been used in Astronomy for a number of data analysis tasks like scheduling observations (Johnston, Adorf 1992), adaptive optics (Angel et al. 1990), stellar spectral classification (Gulati et al. 1994; von Hippel et al. 1994), and star–galaxy separation studies (Odewahn et al. 1992). In addition Gulati, Gupta, and Rao (1997a) extended the ANN analysis to compare synthetic and observed spectra of G and K dwarfs. Gulati, Gupta, and Singh (1997b) estimated interstellar extinction $E(B-V)$ using ANN from low-dispersion ultraviolet spectra for O and B stars. Bailer-Jones, Gupta, and Singh (2002) provide a review of the ANN applications in astronomical spectroscopy.

Another powerful statistical tool for data analysis is the

Table 1. ANN training and test cases.*

Case	Training (Library, number of spectra)	Testing (Library, number of spectra)	λ Region	Resolution	Classification error
A1	JHC, 158	CFLIB, 1273	4100–5500 Å	4.5 Å	674.3
A2	JHC, 158	ELODIE, 1959	4100–5500 Å	4.5 Å	514.8
A3	JHC, 158	STELIB, 247	3600–7400 Å	4.5 Å	861.2
B1	ELODIE, 174	ELODIE, 1959	4000–5500 Å	1 Å	496.4
B2	ELODIE, 174	ELODIE, 1959	4000–6800 Å	1 Å	576.0
B3	ELODIE, 174	CFLIB, 1272	4000–5500 Å	1 Å	742.7
B4	ELODIE, 174	CFLIB, 1273	4000–6800 Å	1 Å	848.5
C1	STELIB, 247	CFLIB, 1273	4000–6800 Å	3 Å	643.9
C2	STELIB, 247	CFLIB, 1273	3500–9400 Å	3 Å	670.6
C3	STELIB, 247	ELODIE, 1959	4000–6800 Å	3 Å	501.8

* Two hidden layers were used for all the cases.

principal component analysis (PCA). It involves a mathematical procedure that transforms a number of (possibly) correlated variables into a (smaller) number of uncorrelated variables called principal components. The first principal component accounts for as much of the variability in the data as possible, and each succeeding component accounts for as much of the remaining variability as possible. Objectives of principal component analysis are to discover or to reduce the dimensionality of a data set and to identify new meaningful underlying variables. The technique has been used widely for a number of applications in Astronomy, viz., for stellar classification by Murtagh and Heck (1987), Storrie-Lombardi et al. (1994), and Singh et al. (1998), by Francis et al. (1992) for QSO spectra, and for galaxy spectra by Sodré and Cuevas (1994), Connolly et al. (1995), Lahav et al. (1996), and Folkes, Lahav, and Maddox (1996).

Another important application was developed by Unno and Yuasa (1992, 2000) for supplementing missing observational data using a generalized PCA technique. Subsequently, Yuasa, Unno, and Magono (1999) made use of this technique to determine distances of 183 mass-losing red giants.

The primary aim of this paper is to perform validity checks on the CFLIB by running the ANN code on various inter library sets like JHC, ELODIE, and STELIB. In the next section we describe the ANN analysis. In section 3, we demonstrate the possibility of using PCA for filling the gaps in the spectra of CFLIB. In section 4, we summarize important conclusions of the study.

2. ANN Analysis

A classification scheme using ANN involves two stages: a training stage and a testing stage. In the training stage, the input patterns and the desired output patterns are defined before the learning process of the ANN is carried out. During training, the network output and the desired output are compared and the network weights are adjusted. We employ a back propagation algorithm (Rumelhart et al. 1986) to achieve this. The learning is stopped when the desired error threshold is reached and the network weights are frozen for use with the test set. In the testing stage, the test patterns are used by the network and classified in terms of the training classes.

In what follows, we have trained the ANN on three libraries with a view to run validity checks on the CFLIB. Three libraries that we used for training are:

1. JHC (Jacoby et al. 1984) with 158 spectra available in the range of 3510–7427 Å at 4.5 Å resolution
2. ELODIE (Moultaka et al. 2004) with 1959 spectra in the range of 4000–6800 Å at a resolution of 0.55 Å
3. STELIB (Le Borgne et al. 2003) with 247 spectra in the range of 3200–9500 Å at 3 Å resolution

A total of 10 test cases were run and are summarized in table 1. We also give the wavelength region used in each case, resolution, and the resulting classification error. Cases A1–A3 involved training of the ANN by JHC and testing on, respectively, the CFLIB, ELODIE, and STELIB. Cases B1–B4 involved training the ANN with 174 individual classes of ELODIE and testing on ELODIE (4000–5500 Å, Case B1), ELODIE (4000–6800 Å, Case B2), CFLIB (4000–5500 Å, Case B3), and CFLIB (4000–6800 Å, Case B4). The last three cases C1–C3 involved training on STELIB and testing on CFLIB (4000–6800 Å, Case C1), CFLIB (3500–9400 Å, Case C2), and ELODIE (4000–6800 Å, Case C3).

The resolution used for training and testing for cases A1–A3 is 4.5 Å which is the resolution of JHC, 1 Å for cases B1–B4 which is the resolution of CFLIB, and 3 Å for cases C1–C3 which is the resolution of STELIB. The higher resolutions of some of the testing cases were degraded to match the resolution of the training library by Gaussian convolution. The testing is done on the complete libraries, i.e., for 247 stars of STELIB, 1959 stars of ELODIE, and 1273 stars of CFLIB.

The classification scatter plots from these analyses are shown in figures 1–3. The MK spectral types have been coded numerically for use by the ANN. The MK alphabetic type O is given a numeric code of 1000, B is 2000, A is 3000, and so on with M being 7000. The subclasses are multiplied by 100 and added in, thus an F5 star is coded as 4500. The luminosity

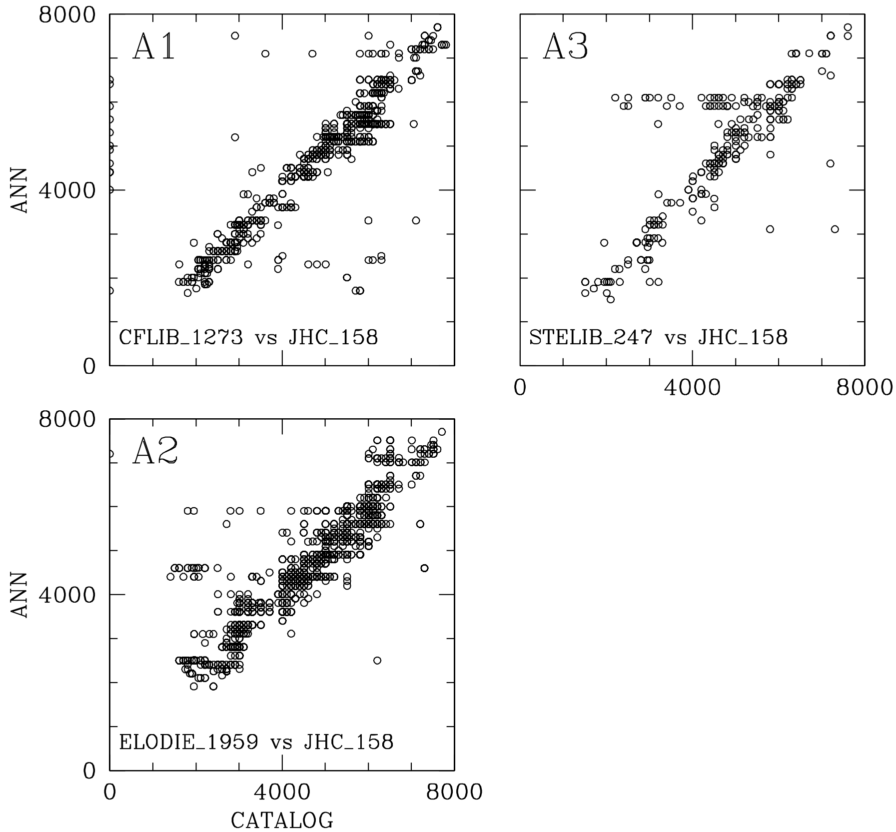

Fig. 1. Classification scatter plots for Cases A1–A3. Expression by numbers in axes for classification is referred to the text.

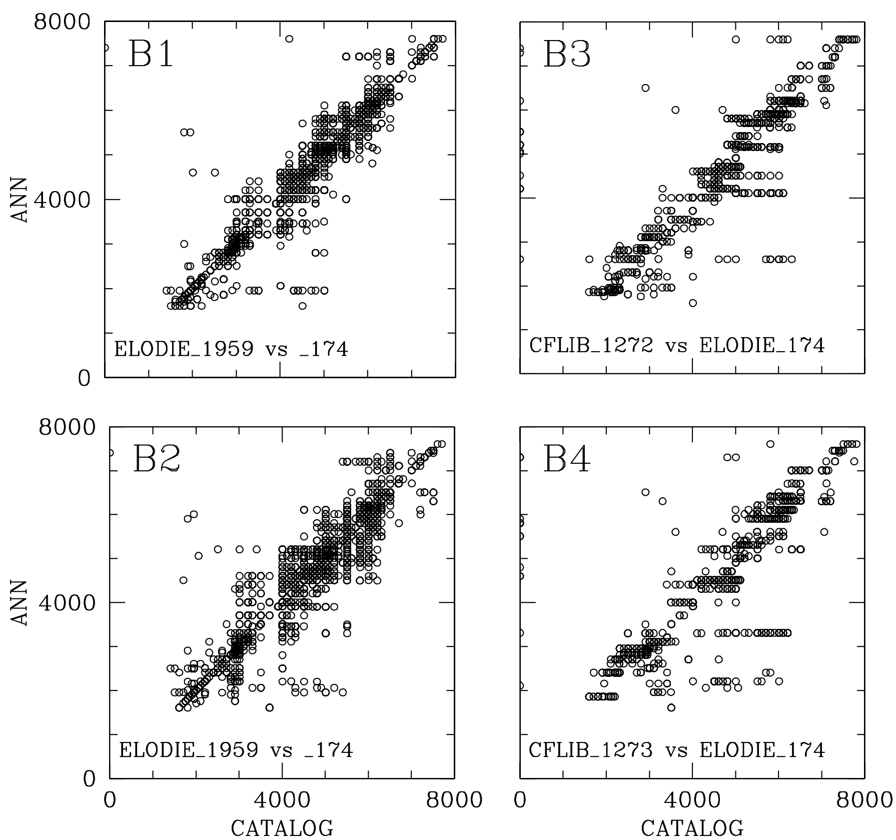

Fig. 2. Classification scatter plots for Case B1–B4.

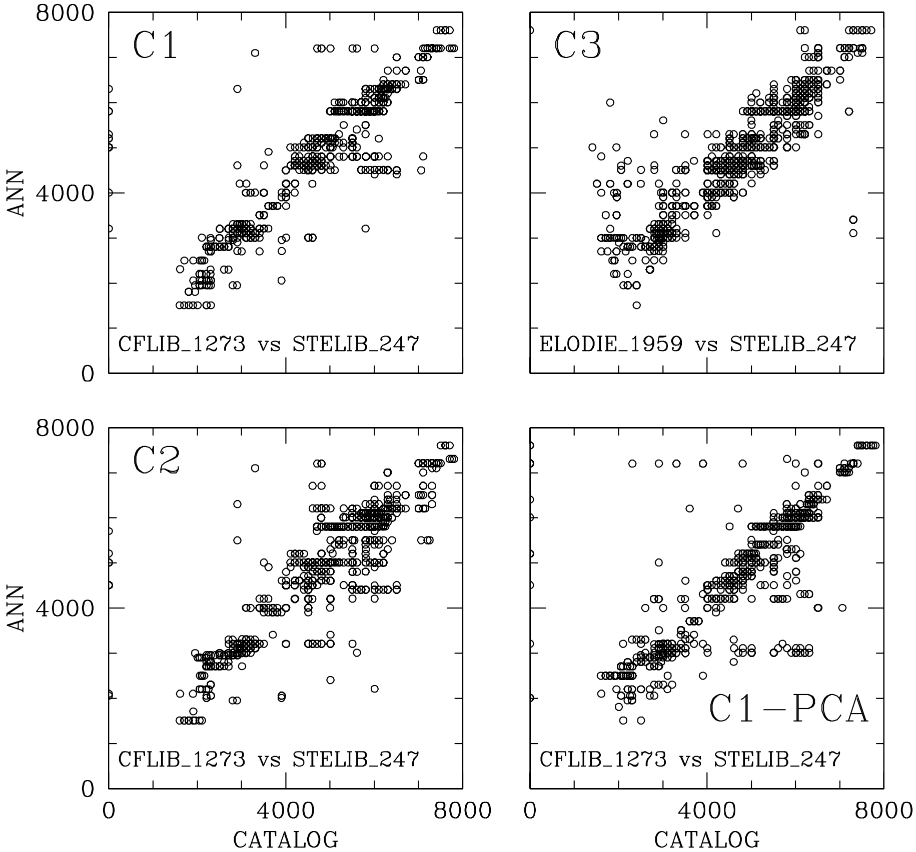

Fig. 3. Classification scatter plots for Case C1–C3. Also shown is case C1 with PCA preprocessing where first 15 principal components were used.

classes I, II, III, IV, and V are coded as 1.5, 3.5, 5.5, 7.5, and 9.5, respectively. An F5 V star is thus coded as 4509.5. In the present scheme, the luminosity class is given a low weight and the main emphasis on classification of the spectral types.

In the following we provide a discussion on the classification accuracy of the three sets of cases:

Cases A1–A3

The Cases A1–A3 use JHC as the training set with A1 and A2 in the wavelength region 4100–5500Å, i.e., in the blue part of the spectrum. In the case A3, JHC was trained for the full span i.e. 3600–7400 Å and tested on STELIB in the same band. The blue region classification error is lowest for ELODIE and somewhat inferior for CFLIB. However, the full span classification of STELIB deteriorates the error to about 861, i.e., 8.6 sub-spectral-type.

Cases B1–B4

In Case B1–B4, ELODIE was used as the training set and was tested on both ELODIE and CFLIB in the blue and full span. The training set of 174 spectra was preselected from amongst the 1959 ELODIE full set with one example spectra per spectro–luminosity class. The best classification is obtained for the case B1 with blue region of ELODIE. For the same region of CFLIB, i.e., case B2, the classification is somewhat inferior. The full span classification case B3 for ELODIE and case B4 for CFLIB are consequently with higher classification errors.

Cases C1–C3

Cases C1–C3 use STELIB as the training set and the test sets are CFLIB limited span C1, ELODIE limited span C3, and CFLIB full span case C2. The limited span cases of C1 and C3 show errors of 6.43 and 5.01 sub-spectral types but remarkably the case C2 with full span shows an error of only 6.7.

The most useful result as far as CFLIB is concerned, is the case C2 since the largest wavelength span is used for this case. It may be noted that except JHC, all other spectral libraries have gaps in them and this contributes greatly into the classification errors. Further, we also used a PCA based preprocessor for all the cases to reduce the dimensionality of the train–test sets as described in Singh et al. (1998). The resulting classification errors using first 15 principal components are only marginally poorer than the ones listed in the last column of table 1. Last panel in figure 3 shows the scatter plot of case C1 with PCA.

Figure 4 displays some example learning curves of the ANN training sessions for Cases A3, B2–B4, C1–C3, and a PCA version of C1–C3. The B2–B4 (and C1–C3) are same training sessions. All the learning curves fall to a low rms learning error at the level on number of iterations of 30000. The PCA version however requires much less number on iterations (~ 10000) to bring down these errors.

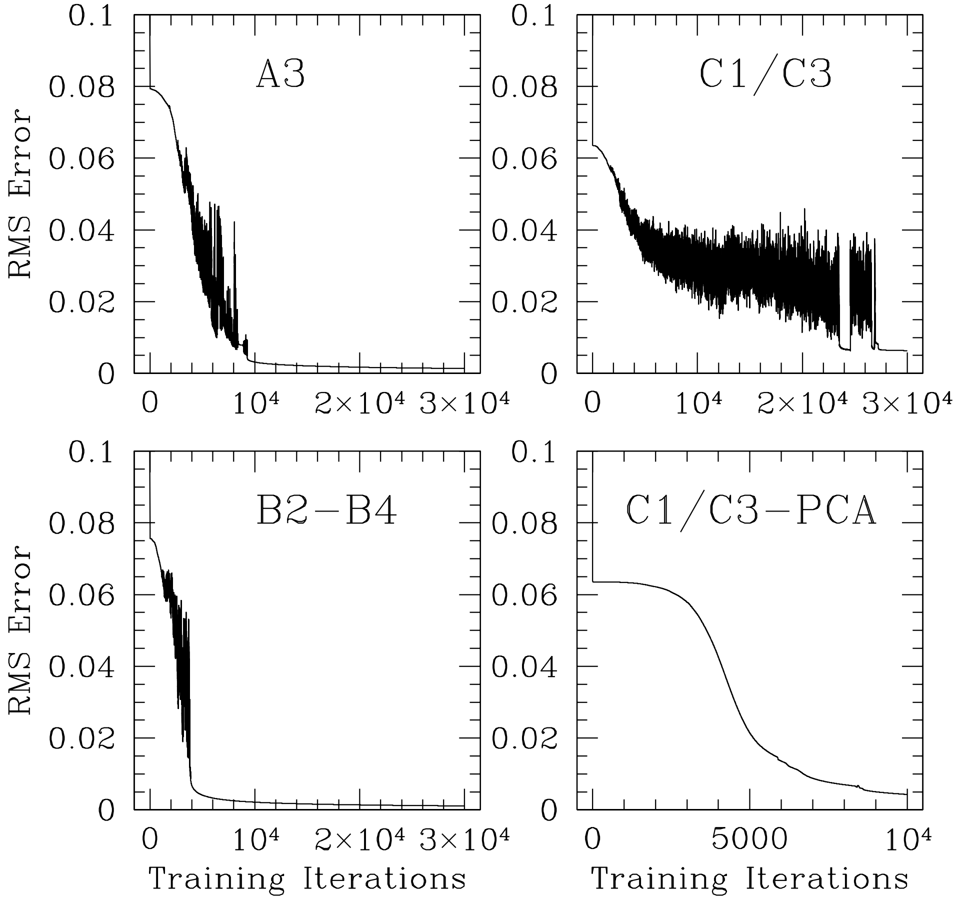

Fig. 4. ANN training session learning curves for some selected cases.

3. Restoration of Missing Data Using PCA

To fill the gaps in the spectra one can use the data from a similar type star which doesn't have a gap at the same wavelength. However, we present here a preliminary study of an automated method for restoration of missing data for a set of spectra of 300 stars in the wavelength region 4000–4300 Å selected from the CFLIB. The list of stars with their spectral types is given in table 3 in Appendix. The method of restoration is adopted from Unno and Yuasa (1992) and is briefly described here for the present data set.

To begin with, we have 301 flux values at 1 Å interval in the range for 4000–4300 Å for 300 stars. A sample of seven spectra are shown in figure 5. For the i-th star, let F_j^i and w_j^i be the j-th observed flux value and its weight respectively, where $j = 1, \dots, n$ $(n = 301)$ and $i = 1, \dots, N$ $(N = 300)$. If a particular flux value F_j^i for a particular star is missing, its weight is equal to zero.

For applying the PCA, the normalized data f_j^i is defined as

$$f_j^i = \frac{\left[F_j^i - \langle F_j \rangle\right]}{\sigma_j}, \tag{1}$$

where $\langle F_j \rangle$ and σ_j are the mean and the standard deviation of F_j respectively and are given by

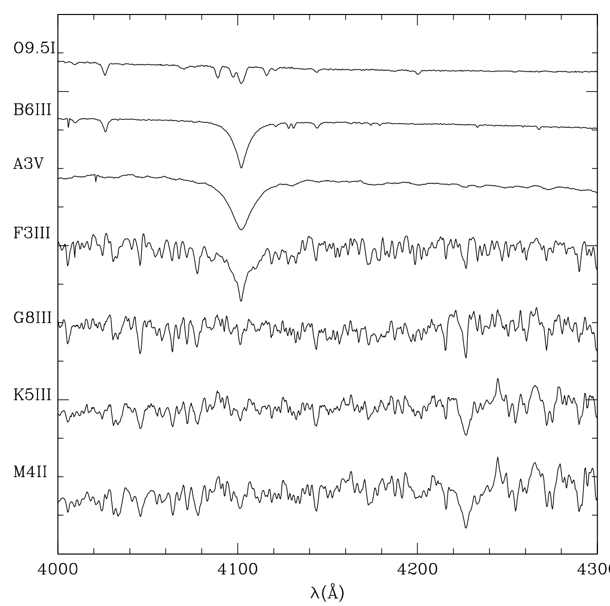

Fig. 5. Representative spectra of seven stars out of the total of 300 stars. The spectral types are listed on the vertical axis.

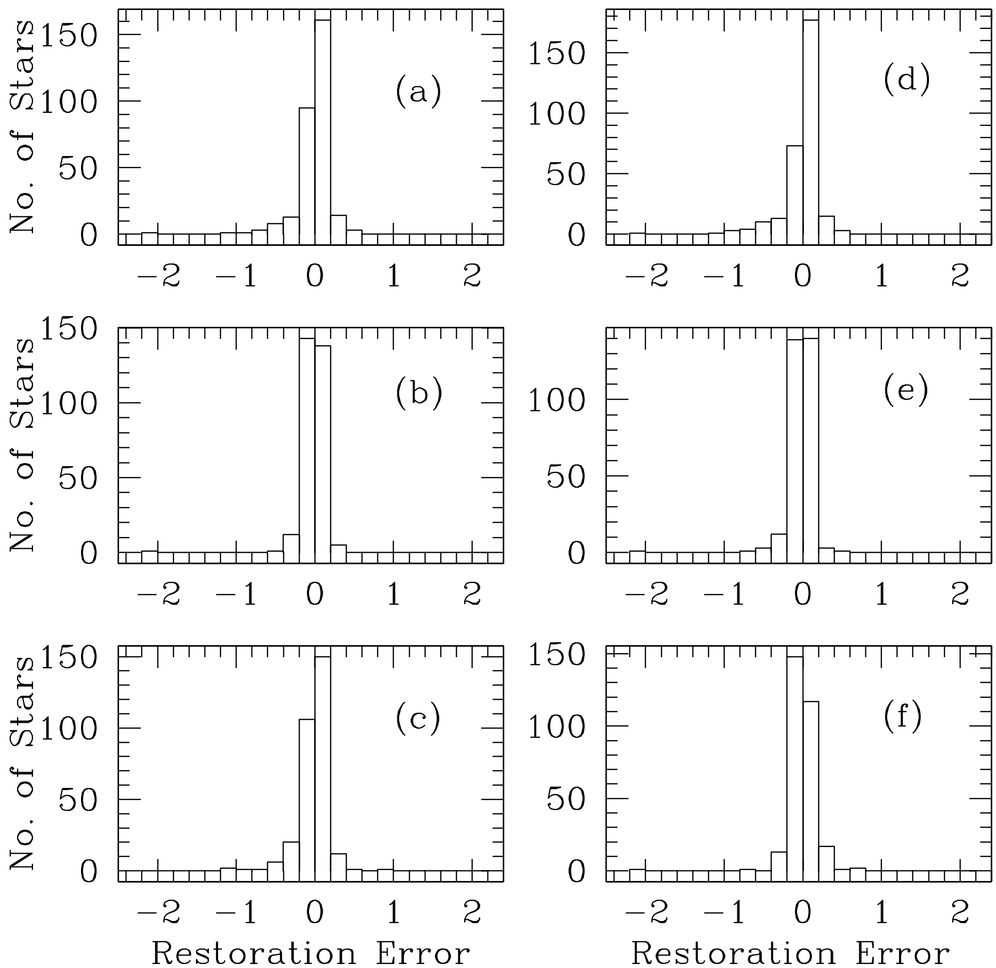

Fig. 6. Histogram of restoration error and the number of stars for the six cases. All stars with restoration errors greater than ±0.2 are binned together.

$$\langle F_j \rangle = \frac{\sum_{i=1}^{N} w_j^i F_j^i}{\sum_{i=1}^{N} w_j^i}, \tag{2}$$

and

$$\sigma_j^2 = \frac{\sum_{i=1}^{N} w_j^i \left[F_j^i - \langle F_j \rangle\right]^2}{\sum_{i=1}^{N} w_j^i}. \tag{3}$$

Following Unno and Yuasa (1992), we define virtual data x_j^i and their corresponding weight v_j^i for each observed flux value f_j^i for each star as

$$v_j^i = 1 - w_j^i, \tag{4}$$

$$\sum_{i=1}^{N} v_j^i x_j^i = 0, \qquad \sum_{i=1}^{N} v_j^i (x_j^i)^2 = \sum_{i=1}^{N} v_j^i. \tag{5}$$

Equation (5) represents the statistical constraint that the mean value of the virtual data is zero and the standard deviation is unity. For such a case, the correlation coefficient between the j-th quantity and the k-th quantity is defined by

$$C_{jk} = \frac{1}{N} \sum_{i=1}^{N} (w_j^i f_j^i + v_j^i x_j^i)(w_k^i f_k^i + v_k^i x_k^i). \tag{6}$$

The most probable value of x_j^i are thus given by the following set of n simultaneous linear algebraic equations:

$$\sum_{l=1}^{n} \frac{1}{\lambda_l} \left[\mu_{lj}^2 x_j^i + \sum_{k \neq j} \mu_{lj} \mu_{lk} (w_k^i f_k^i + v_k^i x_k^i) \right] = 0, \tag{7}$$
$$(j = 1, \ldots, n),$$

where λ_l is the l-th eigenvalue and μ_l^j represent the j-th component of the l-th eigenvector in the PCA. The final adjusted value for the normalized j-th flux value for the i-th star is given by

$$w_j^i f_j^i + v_j^i x_j^i. \tag{8}$$

To check the veracity of this procedure let us assume that from the data set only one flux value F_1^s is missing. This means

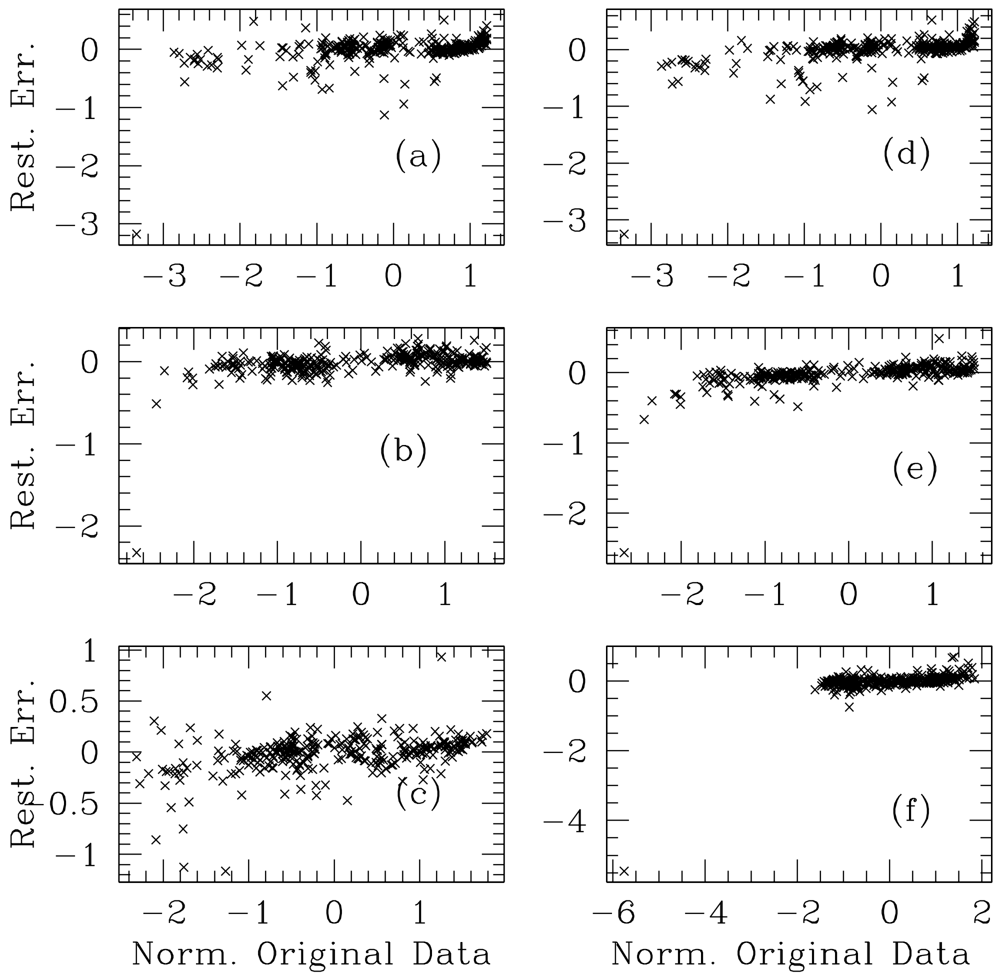

Fig. 7. Restoration error plotted against the normalized original data for all the six cases. The outlier at the bottom left of most of the plots is HD 31996.

Table 2. Cases studied for flux restoration analysis using PCA.

Case	Reconstructed flux	Number of principal components	λ region
(a)	4000 Å	10	4000–4009 Å
(b)	4077 Å	10	4077–4086 Å
(c)	4291 Å	10	4291–4300 Å
(d)	4000 Å	20	4000–4019 Å
(e)	4077 Å	20	4077–4096 Å
(f)	4281 Å	20	4281–4300 Å

that $w_1^s = 0$ and all the other weights w_j^i except w_1^s are equal to unity. In this simplified situation, equations (7) reduce to

$$\left(\sum_{l=1}^{n} \frac{\mu_{l1}^2}{\lambda_l}\right) x_1^s + \sum_{l=1}^{n} \frac{\mu_{l1}}{\lambda_l} \left(\sum_{k=2}^{n} \mu_{lk} f_k^s\right) = 0, \qquad (s = 1, \ldots, N). \tag{9}$$

Equation (9) can be easily solved to get x_1^s for the missing flux f_1^s. By exchanging the columns, one can compute x_2^s, x_3^s, and so on for the missing flux for any wavelength and for any star. Six separate cases were studied and are listed in table 2. The results of our preliminary analysis are shown in figures 6 and 7.

Case (a) uses a flux region of 10 Å starting from 4000 Å and thus 10 principal components to reconstruct the fluxes at 4000 Å for all the 300 stars. From figure 6a we see that 256 stars have restoration error $(f_1^i - x_1^i)$ within ± 0.1. Figure 7a shows the restored error vs. original value of the normalized flux f_1^i (with mean zero). It is clear that for most of the stars the reconstruction is good. Case (d) uses 20 principal components and the reconstruction of flux at 4000 Å is comparable, maybe slightly worse as is clear from figure 6d and figure 7d.

We also tested the validity of this flux reconstruction method by attempting to reproduce a strong absorption feature, namely the 4077 Å Sr II feature, visible in the representative spectra in figure 5. Case (b) attempts to achieve this using 10 principal components rather successfully as is clear from figure 6b and figure 7b respectively. The flux at 4077 Å was reconstructed to within ± 0.1 for a total of 281 stars out of 300. The case (e) with 20 principal components also reproduces the flux at 4077 Å well although no better than case (b) (279 stars within ± 0.1) suggesting that the 10 PC's are enough for the data reconstruction in this data set. Lastly, cases (c) and (f) show similar behavior in reconstructing towards the end of the wavelength interval and the results are plotted in figure 6c and f, and figure 7c and f.

Another interesting offshoot of this analysis was in picking outliers, stars which have either no known MK spectral types or have noisy spectra. Figure 7a,b,d,e,f clearly show one outlier for which our scheme is unable to restore or reconstruct the fluxes. The star is HD 31996 and it indeed has no MK spectral class assigned to it (table 3) as was verified from the CFLIB and the SIMBAD database. Another star, HD 46687, also has no known spectral type but its spectrum resembles an M type star. For this star, our analysis was able to reconstruct the fluxes. The spectra of these two stars obtained from the CFLIB are plotted in figure 8.

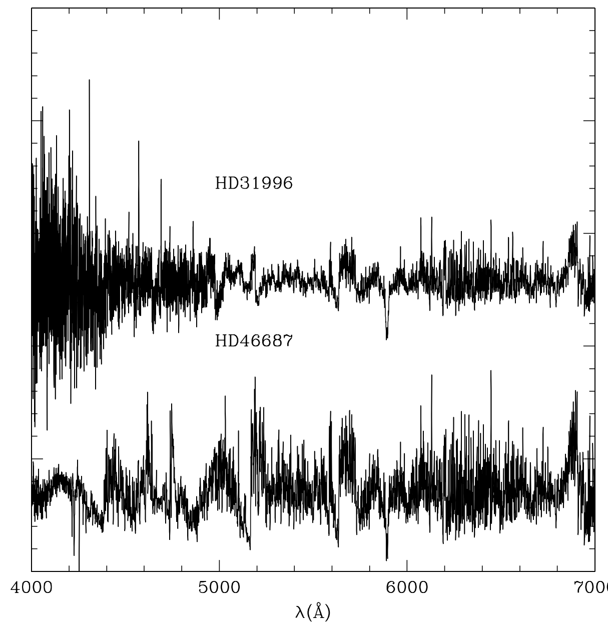

Fig. 8. Spectrum of the two stars HD 31996 and HD 46687 which have no known spectral types. Star HD 31996 is the outlier in the flux restoration analysis.

4. Conclusions

We have performed an extensive analysis based on artificial neural networks to classify stars in an automated manner in the Indo-US CFLIB using three databases viz., JHC, STELIB, and ELODIE. The main aim of this exercise was two-fold. One was to perform the reliability checks on CFLIB to see how the gaps in the library affect the classification accuracy. We find that the despite the presence of gaps, we have achieved classification accuracy of less than one main class. The second aim was to evolve and test automated procedures of classifying stellar spectra. This was achieved by trying our ANN scheme on ten different cases of training and testing on different pairs of libraries. The schemes are numerically intensive, with the ANN training stage requiring several hours of CPU time on the fastest of workstations. A PCA analysis was employed successfully to reduce the dimensionality of the data set and hence faster training without appreciable loss in classification accuracy.

Both STELIB and ELODIE libraries have variable spans of wavelength gaps where the fluxes are filled with zeros (similar to CFLIB). Such gaps lead to classification errors in the PCA and ANN schemes. However, we have carried out some preliminary analysis with the basic χ^2 minimization scheme on these libraries wherein the gap portions were omitted in both train and test sets. This lead to a remarkable improvements in the classification accuracy.

We have also employed a generalized principal component analysis to first create and then fill the gaps in a sample of 300 stars out of the CFLIB in the blue region. At present, we have used a simplified system to reconstruct flux values at one wavelength bin at a time for these 300 stars. We hope to exploit the full potential of the scheme and attempt to fill larger gaps in stellar spectra in a subsequent study.

MY and HPS are grateful to JSPS (Japan Society for Promotion of Science) and DST (Department of Science & Technology, India) for financial support for exchange visits which made this work possible. MY would like to thank Emeritus Professor W. Unno of the University of Tokyo for helpful discussions. The research has made use of the SIMBAD database, operated by CDS, Strasbourg, France and the INDO-US CFLIB managed by NOAO, Tucson, AZ, USA.

Appendix. List of Stars for Data Restoration Analysis

The list of 300 stars with their HD numbers and the spectral types is given in table 3. Two stars HD 31996 and HD 46687 have no known spectral types.

Table 3. Sample of 300 stars used for data restoration analysis.

HD	Sp. type	HD	Sp. type	HD	Sp. type	HD	Sp. type	HD	Sp. type	HD	Sp. type
100889	B9.5 V	141680	G8 III	191615	G8 IV	117818	K0 III	163917	G9 III	43042	F6 V
102212	M1 III	141714	G3.5 III	195324	A1 I	117876	G8 III	163989	F6 IV	43232	K1.5 III
102224	K0.5 III	142091	K1 IV	196867	B9 IV	118055	K0	164259	F2 IV	43247	B9 II
102328	K3 III	142198	K0 III	198001	A1 V	118266	K1 III	164284	B2 V	43318	F6 V
102870	F9 V	142373	F8 V	25329	K1 V	120136	F6 IV	164353	B5 I	43380	K2 III
103047	K0	143107	K2 III	28978	A2 V	120164	K0 III	165029	A0 V	43827	K1 III
103287	A0 V	143666	G8 III	29613	K0 III	120348	K1 III	165358	A2 V	43947	F8 V
104985	G9 III	143761	G0 V	29645	G0 V	120452	K0 III	165401	G0 V	44007	G5 IV
105043	K2 III	145328	K1 III	30562	F8 V	121146	K2 IV	165645	F0 V	44033	K3 I
105262	B9	146791	G9.5 III	30614	O9.5 I	121370	G0 IV	165687	K0 III	44478	M3 III
106365	K2 III	147677	K0 III	30652	F6 V	122563	F8 IV	165760	G8 III	44537	M0 I
106714	G8 III	148387	G8 III	30739	A1 V	123657	M4.5 III	165908	F7 V	44769	A5 IV
107113	F4 V	148783	M6 III	30743	F5 V	123977	K0 III	166014	B9.5 V	44951	K3 III
107213	F8 V	148786	K0 III	30812	K1 III	124570	F6 IV	166046	A3 V	45282	G0
107383	G8 III	149161	K4 III	31295	A0 V	124850	F7 IV	166207	K0 III	45410	K0 III
107418	K0 III	149630	B9 V	31421	K2 III	124897	K1.5 III	167042	K1 III	45412	F8 I
107950	G6 III	149661	K2 V	31996	0.0	125451	F5 IV	168151	F5 V	46184	K1 III
108225	G9 III	149757	O9 V	32147	K3 V	125454	G8 III	168656	G8 III	46687	0.0
108954	F9 V	150012	F5 IV	33111	A3 III	126141	F5 V	168723	K0 III	47105	A0 IV
109317	K0 III	150100	B9.5 V	33256	F2 V	126271	K4 III	169191	K3 III	47205	K1 III
109345	K0 III	150117	B9 V	35468	B2 III	126868	G2 IV	169414	K2 III	47731	G5 I
109358	G0 V	150449	K1 III	35497	B7 III	127334	G5 V	170693	K1.5 III	47839	O7 V
110281	K5	150453	F3 V	36673	F0 I	128000	K5 III	171301	B8 IV	48329	G8 I
110897	G0 V	150680	G0 IV	36861	O8 III	128750	K2 III	171391	G8 III	48432	K0 III
111335	K5 III	150997	G7.5 III	37043	O9 III	129312	G7 III	172569	F0 V	48433	K1 III
111591	K0 III	151431	A3 V	37160	K0 III	129336	G8 III	173087	B5 V	48737	F5 IV
111765	K4 III	151613	F2 V	37984	K1 III	129956	B9.5 V	173399	G5 IV	48781	K1 III
111812	G0 III	151769	F7 IV	38656	G8 III	129972	G8.5 III	175317	F6 IV	50420	A9 III
112300	M3 III	151862	A1 V	38899	B9 IV	129978	K2 III	175535	G7 III	51309	B3 I
113226	G8 III	152569	F0 V	39003	G9.5 III	130948	G1 V	175545	K2 III	54662	O7 III
113436	A3 V	152614	B8 V	39283	A2 V	131111	K0 III	175588	M4 II	54719	K2 III
113848	F4 V	152815	G8 III	39587	G0 V	131156	G8 V	175640	B9 III	55280	K2 III
113996	K5 III	15318	B9 III	39801	M1	132132	K1 III	175743	K1 III	55575	G0 V
114038	K1 III	153597	F6 V	39853	K5 III	132345	K3 III	175751	K2 III	57264	G8 III
114092	K4 III	153653	A7 V	39866	A2 II	133165	K0.5 III	176301	B7 III	57669	K0 III
114330	A1 IV	153808	A0 V	40035	K0 III	133208	G8 III	176318	B7 IV	57727	G8 III
114357	K3 III	154278	K1 III	40111	B0.5 II	134083	F5 V	176582	B5 IV	58207	G9 III
114642	F6 V	154431	A5 V	40136	F1 V	134190	G7.5 III	176819	B2 IV	58343	B2 V
114710	F9.5 V	154445	B1 V	40183	A2 IV	135742	B8 V	177724	A0 V	58551	F6 V
115004	K0 III	154660	A9 V	40239	M3 II	136064	F9 IV	177817	B7 V	59881	F0 III
115136	K2 III	155763	B6 III	40536	A6	136202	F8 III	178125	B8 III	60179	A1 V
115202	K1 III	157741	B9 V	40801	K0 II	136512	K0 III	178329	B3 V	61064	F6 III
115383	G0 V	157910	G5 III	41117	B2 I	136726	K4 III	180006	G8 III	61295	F6 II
115539	G8 III	158716	A1 V	41330	G0 V	137052	F5 IV	180711	G9 III	62509	K0 III
115604	F3 III	158899	K4 III	41597	G8 III	138716	K1 IV	182293	K3 IV	63302	K3 I
115617	G5 V	159332	F6 V	41636	G9 III	139195	K0 III	182568	B3 IV	65714	G8 III
116292	K0 III	160765	A1 V	41692	B5 IV	139446	G8 III	183144	B4 III	65900	A1 V
116656	A2 V	161056	B1.5 V	42475	M1 I	139641	G7.5 III	184915	B0.5 III	67228	G1 IV
117176	G5 V	161868	A0 V	42543	M1 I	140027	G8 III	188350	A0 III	69897	F6 V
117243	G5 III	163588	K2 III	43039	G8.5 III	141004	G0 V	191243	B5 I	70110	F9 V

References

Angel, J. R. P., Wizinowich, P., Lloyd-Hart, M., & Sandler, D. 1990, Nature, 348, 221

Bailer-Jones, C. A. L., Gupta, R., & Singh, H. P. 2002, in Automated Data Analysis in Astronomy, ed. R. Gupta, H. P. Singh, & C. A. L. Bailer-Jones (New Delhi: Narosa), 51

Cenarro, A. J., Cardiel, N., Gorgas, J., Peletier, R. F., Vazdekis, A., & Prada, F. 2001, MNRAS, 326, 959

Connolly, A. J., Szalay, A. S., Bershady, M. A., Kinney, A. L., & Calzetti, D. 1995, AJ, 110, 1071

Folkes, S. R., Lahav, O., & Maddox, S. J. 1996, MNRAS, 283, 651

Francis, P. J., Hewett, P. C., Foltz, C. B., & Chaffee, F. H. 1992, ApJ, 398, 476

Gulati, R. K., Gupta, R., Gothoskar, P., & Khobragade, S. 1994, ApJ, 426, 340

Gulati, R. K., Gupta, R., & Rao, N. K. 1997a, A&A, 322, 933

Gulati, R. K., Gupta, R., & Singh, H. P. 1997b, PASP, 109, 843

Jacoby, G. H., Hunter, D. A., & Christian, C. A. 1984, ApJS, 56, 257 (JHC)

Johnston, M. D., & Adorf, H.-M. 1992, Comput. Operations Res., 19, 209

Lahav, O., Naim, A., Sodré, L., Jr., & Storrie-Lombardi, M. C. 1996, MNRAS, 283, 207

Le Borgne, J.-F., et al. 2003, A&A, 402, 433 (STELIB)

Moultaka, J., Ilovaisky, S. A., Prugniel, P., & Soubiran, C. 2004, PASP, 116, 693 (ELODIE)

Murtagh, F., & Heck, A. 1987, Multivariate Data Analysis (Dordrecht: Reidel)

Odewahn, S. C., Stockwell, E. B., Pennington, R. L., Humphreys, R. M., & Zumach, W. A. 1992, AJ, 103, 318

Prugniel, Ph., & Soubiran, C. 2001, A&A, 369, 1048

Rumelhart, D. E., Hinton, G. E., & Williams, R. J. 1986, Nature, 323, 533

Singh, H. P., Gulati, R. K., & Gupta, R. 1998, MNRAS, 295, 312

Sodré, L., Jr., & Cuevas, H. 1994, Vistas Astron., 38, 287

Storrie-Lombardi, M. C., Irwin, M. J., von Hippel, T., & Storrie-Lombardi, L. J. 1994, Vistas Astron., 38, 331

Unno, W., & Yuasa, M. 1992, Ap&SS, 189, 271

Unno, W., & Yuasa, M. 2000, PASJ, 52, 127

Valdes, F., Gupta, R., Rose, J. A., Singh, H. P., & Bell, D. J. 2004, ApJS, 152, 251 (CFLIB)

von Hippel, T., Storrie-Lombardi, L. J., Storrie-Lombardi, M. C., & Irwin, M. J. 1994, MNRAS, 269, 97

Yuasa, M., Unno, W., & Magono, S. 1999, PASJ, 51, 197